Chemistry & Biology
Article

Binding Specificity of Retinal Analogs to Photoactivated Visual Pigments Suggest Mechanism for Fine-Tuning GPCR-Ligand Interactions

Sundaramoorthy Srinivasan,[1] Eva Ramon,[1] Arnau Cordomí,[2] and Pere Garriga[1,*]
[1]Chemical Engineering Department, Grup de Biotecnologia Molecular i Industrial, Centre de Biotecnologia Molecular, Universitat Politècnica de Catalunya, Edifici Gaia, Rambla de Sant Nebridi 22, 08222 Terrassa, Catalonia, Spain
[2]Laboratori de Medicina Computacional, Unitat de Bioestadística, Facultat de Medicina, Universitat Autònoma de Barcelona, 08193 Bellaterra, Barcelona, Spain
*Correspondence: pere.garriga@upc.edu
http://dx.doi.org/10.1016/j.chembiol.2014.01.006

SUMMARY

11-*cis*-retinal acts as an inverse agonist stabilizing the inactive conformation of visual pigments, and upon photoactivation, it isomerizes to all-*trans*-retinal, initiating signal transduction. We have analyzed opsin regeneration with retinal analogs for rhodopsin and red cone opsin. We find differential binding of the analogs to the receptors after photobleaching and a dependence of the binding kinetics on the oligomerization state of the protein. The results outline the sensitivity of retinal entry to the binding pocket of visual receptors to the specific conformation adopted by the receptor and by the molecular architecture defined by specific amino acids in the binding pocket and the retinal entry site, as well as the topology of the retinal analog. Overall, our findings highlight the specificity of the ligand-opsin interactions, a feature that can be shared by other G-protein-coupled receptors.

INTRODUCTION

Light-induced isomerization of 11-*cis*-retinal (11CR) to all-*trans*-retinal (ATR) triggers a conformational change in visual receptors, resulting in the formation of their active states and initiating the complex process of vision (Schoenlein et al., 1991; Wald, 1968). These visual pigments belong to the G-protein-coupled receptor (GPCR) superfamily and consist of a heptahelical transmembrane (TM) apoprotein, opsin, covalently linked to its natural chromophore, 11CR, a vitamin A derivative (Palczewski et al., 2000). Photoreceptor cells are classified as the much-abundant rod cells and the scarcer cone cells, which are responsible for scotopic and photopic vision, mediated by rhodopsin and cone opsins, respectively (Shichida and Imai, 1998).

The 11CR chromophore has been conserved throughout evolution, because of its highly specialized role in vision, which includes a high quantum yield and a very fast response for photon-triggered isomerization. Retinal analogs, other than the natural 11-*cis* chromophore, such as 7-*cis*, 9-*cis*, 13-*cis*, and all-*trans*, have been investigated for their binding properties to the visual pigments in order to unravel the structural features of the retinal binding site and the details of the opsin-ligand recognition process (Schick et al., 1987; Harbison et al., 1984; Fukada et al., 1990). 9-*cis*-retinal (9CR) is often used as an exogenous analog to study the structure and function of native rhodopsin (Hubbard and Wald, 1952; Nakamichi and Okada, 2007).

The main feature used to distinguish these visual pigments, bound to a particular chromophore, from each other is their wavelength of maximal absorption in the visible region of the electromagnetic spectrum. In mammalian natural pigments with 11CR, these correspond to 500 nm (rhodopsin), 420 nm (short-wavelength-sensitive pigment or blue cone pigment), 530 nm (middle-wavelength-sensitive pigment or green cone pigment), and 560 nm (long-wavelength cone pigment or red cone pigment) (Kakitani et al., 1985; Merbs and Nathans, 1992; Neitz et al., 1991). Metarhodopsin II (MetaII) is the active conformation of the visual pigments formed upon photoactivation, in which the chromophore is still covalently bound to the opsin apoprotein. The presence of this covalent bond, though it is not strictly required (Zhukovsky et al., 1991), is important for the optimal functionality of the receptor (Matsuyama et al., 2010). The isomerized chromophore eventually destabilizes the conformation of the pigments, causing breakage of this bond and yielding opsin plus free ATR, which leaves the retinal binding pocket (Bartl et al., 2005).

In the dark, the aldehyde group of 11CR is covalently bound to the receptor via a protonated Schiff-base linkage with K296$^{7.43}$ of rhodopsin/blue cone opsin or K312$^{7.43}$ of red/green cone opsin (superscripts refer to the general numbering system for GPCRs; Ballesteros and Weinstein, 1995), thereby maintaining the inactive conformation (Mustafi et al., 2009; Palczewski et al., 2000). The fluorescence emission of W265/281$^{6.48}$, which is located very close to the β-ionone ring of the retinal, and W126/142$^{3.41}$ (Hoersch et al., 2008) are quenched by bound retinal of these dark-adapted visual pigments. Hydrolysis of the retinylidene linkage by photoisomerization causes the release of retinal and the parallel increase in fluorescence due to the fact that these tryptophan residues, particularly W265/281$^{6.48}$ (Farrens and Khorana, 1995), are no longer quenched. Therefore, we have used fluorescence spectroscopy to follow both the retinal release and uptake processes for these visual pigments.

In rhodopsin and cone opsins, photoactivation-induced conformational changes result in an activated receptor binding to transducin, the specific heterotrimeric G protein. Binding of the pigment to transducin causes exchange of GDP to GTP,

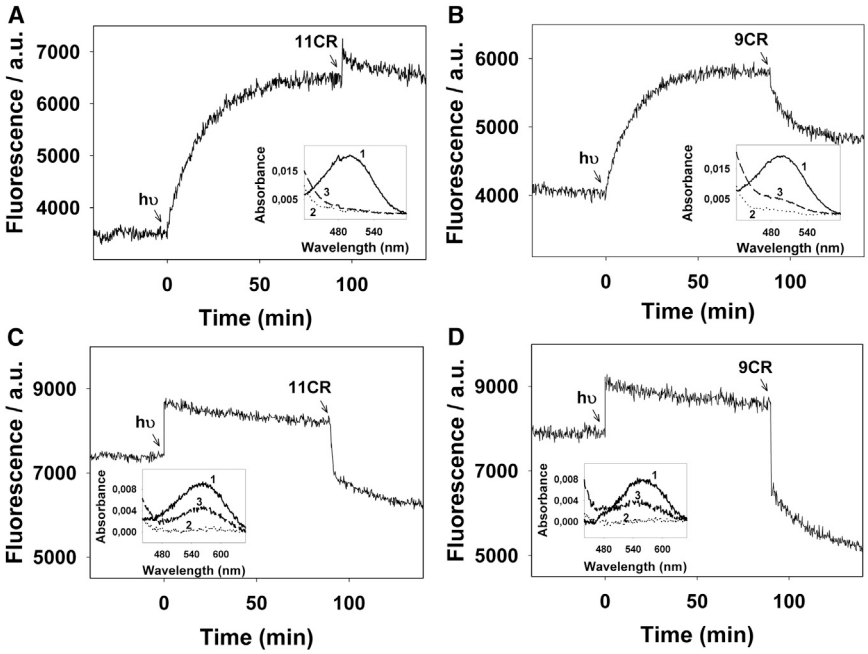

Figure 1. Photoactivated Visual Pigment Regeneration with Retinal Analogs

Purified recombinant rhodopsin added to the microcuvette was illuminated for 30 s (>495 nm) after the dark-state spectra stabilized.

(A and B) A 2.5-fold of 11CR/9CR to the concentration of rhodopsin sample was added and mixed well. Regeneration was also followed by UV-visible spectroscopy on the same fluorimetric samples (inset, A and B: 1, dark; 2, illuminated; 3, regenerated).

(C and D) Analogous to rhodopsin, red cone opsin was illuminated (>495 nm) after the stable baseline dark-state spectrum was obtained, followed by 11CR/9CR addition. UV-visible spectroscopy of dark-state red cone opsin was also measured as in the rhodopsin case (inset C and D: 1, dark; 2, illuminated; 3, regenerated).

activating its α subunit and, after dissociation from the βγ complex, triggering its binding and activation of a cGMP phosphodiesterase (Schertler, 2008). Cone opsins show lower sensitivity to light than does rhodopsin, which allows rhodopsin to mediate dim light vision, whereas cone opsins mediate bright daylight vision (Kawamura and Tachibanaki, 2008). The rate of transducin activation by cone opsins was found to be significantly different from that of rhodopsin (Imai et al., 1997).

We have previously reported the effect of different factors, like salts or lipids, on the structure and function of rhodopsin (Reyes-Alcaraz et al., 2011; Sánchez-Martín et al., 2013; Toledo et al., 2009), as well as the biochemical features of rhodopsin mutations associated with the retinal degenerative disease retinitis pigmentosa (Ramon et al., 2003; Toledo et al., 2011). In the present work, we aimed at describing chromophore regeneration with 9CR and 11CR after photoactivation—and MetaII decay—of red cone opsin and rhodopsin. Our results show that purified red cone opsin allows regeneration with 11CR and 9CR after photobleaching, whereas rhodopsin is only able to bind 9CR. This suggests that the retinal binding site of red cone opsin is more accessible than that of rhodopsin. Our current data also indicate that this regeneration process may be modulated by the formation of receptor oligomers. Molecular modeling provides a structural basis supporting our spectroscopic results, which highlight the fine-tuning and specificity of ligand-receptor interactions for rhodopsin-like GPCRs. This specificity and conformational complementarity may have general implications for other members of the GPCR superfamily.

RESULTS

Only 9CR Can Access the Rhodopsin Binding Pocket at the Post-Meta II Phase

Upon illumination of purified rhodopsin, an increase in Trp fluorescence is observed due to the retinal release from its binding pocket (Figure 1A) that closely parallels the MetaII decay process under the present experimental conditions. The fluorescence curve can be fit to a single exponential function with $t_{1/2}$ ~15 min in agreement with previously published data (Reyes-Alcaraz et al., 2011). The addition of 11CR ~90 min after photobleaching (after complete decay of MetaII) did not decrease Trp fluorescence, indicating that 11CR is not able to reach the binding pocket (Figure 1A). On the other hand, the addition of 9CR resulted in a decrease of the fluorescence signal compatible with the presence of the exogenously added retinal in the binding pocket (Figure 1B). Control assays were carried out to rule out contribution of the buffer and other factors to the observed protein behavior (see Figures S1 and S2 available online).

We also performed an experiment in which 9CR was previously mixed with hydroxylamine before being added to the photobleached rhodopsin sample. In this case we observed a fast decrease in fluorescence (Figure S3), suggesting that 9CR could enter the binding pocket without formation of a Schiff base linkage. Different kinetics could be observed when only 9CR was added to the sample (Figure S3).

Parallel experiments, carried out using UV-visible spectroscopy under identical experimental conditions to those of fluorescence assay, showed the presence of the 500 nm band indicating regeneration of photobleached opsin. No regeneration was observed with 11CR (Figure 1A, inset), whereas ~25% regeneration could be detected with 9CR (Figure 1B, inset). These results are in agreement with the fluorescence measurements and prove that retinal binds covalently to opsin. In order to track the loss of 11CR regeneration ability for rhodopsin after photoactivation, the regeneration experiment was carried out at different time points (0, 30, and 60 min). The spectroscopic analysis showed a minimal regeneration at 30 min after photoactivation, which is virtually abolished at 60 min. In the case of 9CR, a significant regeneration can be detected throughout this time period (data not shown). These data suggest that opsin stability plays also a role in the observed pigment behavior.

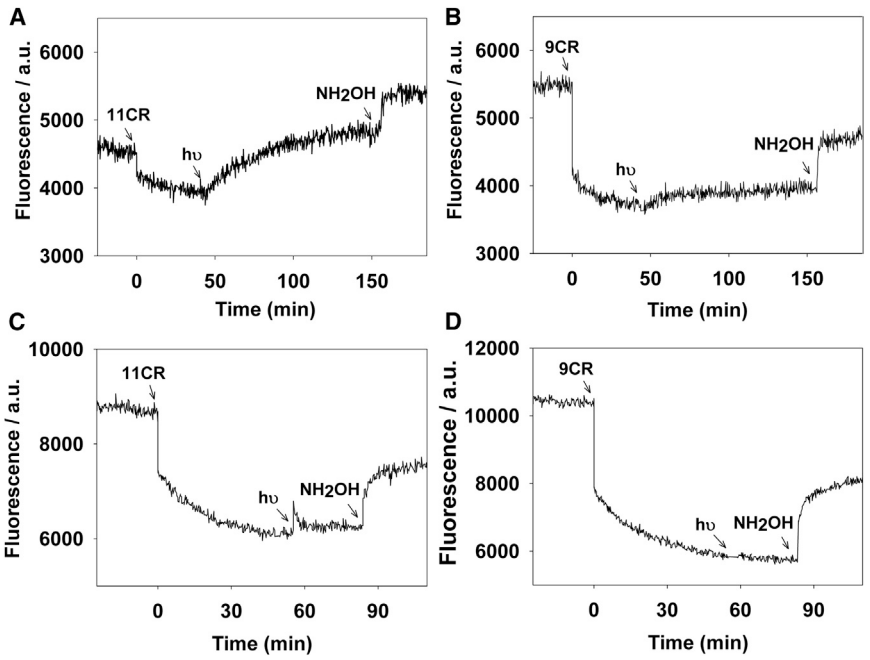

Figure 2. Difference in Accessibility of Retinal Binding Sites of Rhodopsin and Red Cone Opsin with Retinal Analogs

(A and B) 11CR and 9CR (2.5-fold more than the rhodopsin concentration) were added to purified rhodopsin, followed by illumination (>495 nm) and 50 mM hydroxylamine addition in the same sample when the stable spectra was obtained after each treatment.

(C and D) Same experiment was carried out with purified red cone opsin.

11CR and 9CR Can Access the Red Cone Opsin Binding Pocket at the Post-Meta II Phase

An abrupt fluorescence increase is detected upon red cone illumination (Figures 1C and 1D), compatible with a fast retinal release (Chen et al., 2012). Addition of either 11CR or 9CR, after complete retinal release, resulted in a decrease in intensity suggesting that the two analogs could occupy the red cone binding pocket (Figures 1C and 1D). UV-visible spectroscopy showed a typical absorbance band with a maximum at 560 nm indicating red cone chromophore formation. Up to a ~60% of regeneration was observed with both retinals (Figures 1C and 1D, insets). Post-bleaching regeneration showed a two-phase kinetics, which includes a sudden drop in fluorescence, suggesting the fast entry of retinal into the binding pocket, and a slower decaying component, suggesting the actual binding of retinal to the pigment. The fact that the fluorescence signal decreases to a level below that of the original pigment may be due to the presence of nonregenerated opsin resulting from the immunopurification process. In the case of the 9CR, this isomer may be a better quencher than 11CR because of its increased interaction with Trp residues.

Accessibility of Retinal Binding Sites of Rhodopsin and Red Cone Opsin by Retinal Analogs

In order to prove the hypothesis of different accessibility of the two retinal analogs to the binding pocket, we incubated rhodopsin and red cone pigment with 11CR and 9CR, prior to photoactivation, and the fluorescence intensity was monitored (Figure 2A and 2B). We found that there was nearly no change in rhodopsin fluorescence in the dark upon addition of 11CR, whereas after illumination (with light >495 nm), a minimal increase could be detected (Figure 2A). This increase is much smaller than the typical MetaII decay curve (see Figure 1A) and may be due to the presence of an excess amount of 11CR that may replenish the pigment as previously reported (Farrens and Khorana, 1995). Addition of hydroxylamine resulted in a slight increase in fluorescence (Figure 2A). However, in the case of 9CR added to rhodopsin in the dark, an appreciable decrease in fluorescence intensity could be detected (Figure 2B). Illumination only slightly altered the Trp fluorescence, though to a much smaller extent as compared to 11CR. Addition of hydroxylamine considerably increased the retinal release from the rhodopsin binding pocket (Figure 2B).

In the case of red cone pigment, addition of either 11CR or 9CR caused considerable decrease in fluorescence intensity, indicating entry of both retinals into the binding pocket of free opsin. Fluorescence intensity was not affected by illumination, and subsequent treatment with hydroxylamine resulted in a saturation curve with $t_{1/2}$ of ~3 min, suggesting the formation of retinaloxime, which would be released from the red cone pigment (Figures 2C and 2D).

Improvement of Rhodopsin Regeneration with 9CR Using Low-Salt Buffer

In order to determine the possible effect of buffer conditions on rhodopsin regeneration, recombinant rhodopsin was purified with sodium phosphate (NaPi) buffer and photoactivated in the spectrofluorimetric cuvette. The fluorescence increase was measured until it reached a plateau indicating complete MetaII decay, and then 2.5-fold concentration of 9CR (over rhodopsin) was added and mixed well. An immediate decrease in fluorescence intensity was detected after the addition of 9CR, suggesting a faster regeneration of photoactivated rhodopsin (Figure 3A). A parallel sample monitored by UV-visible spectrophotometry showed better regeneration with 9CR (~70%) than in PBS buffer (Figure 3A, inset; compare to inset in Figure 1A). This finding stresses the importance of the buffer on the chromophore regeneration of the pigment.

Blue native polyacrylamide gel electrophoresis (BN-PAGE) was carried out in order to find out whether oligomerization could alter retinal binding to the receptors. Rhodopsin purified using NaPi buffer clearly showed the predominant presence of oligomeric forms (Figure 3B). In contrast, rhodopsin purified using PBS buffer showed the presence of a strong monomeric band and a much less intense dimer band (Figure 3B). SDS-PAGE showed a single monomeric band, for rhodopsin, in both cases with no indication of oligomeric behavior (Figure 3C). The red cone pigment failed to show regeneration in NaPi; this may be

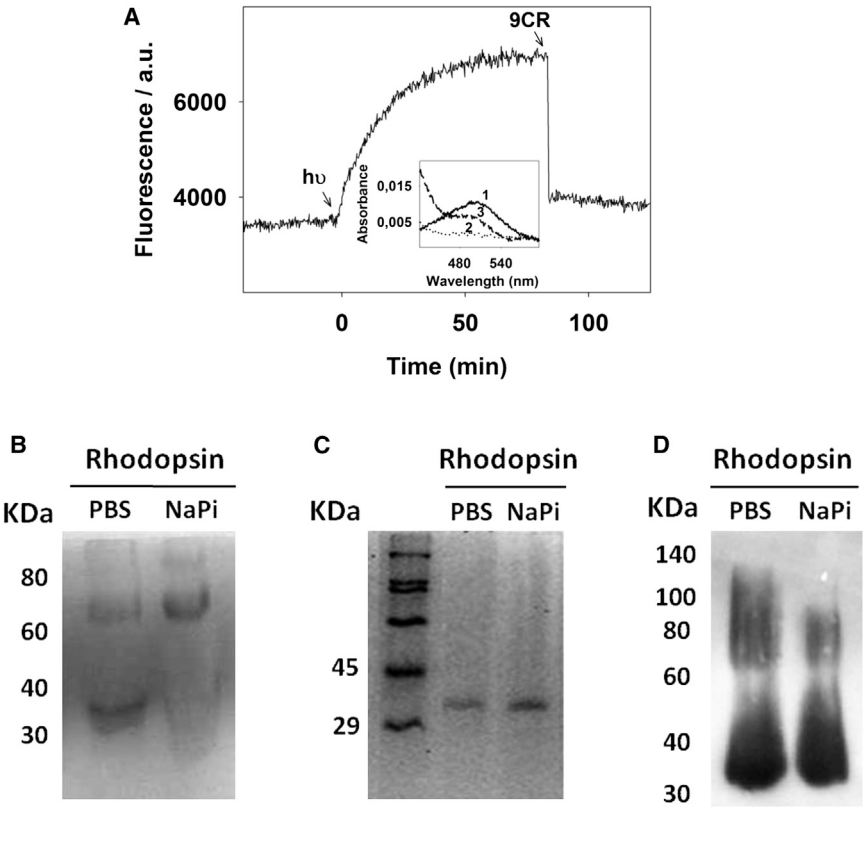

Figure 3. Phosphate Buffer—Low-Salt Conditions—Improves 9CR Regeneration Kinetics of Photoactivated Rhodopsin

Purified recombinant rhodopsin in 2 mM NaPi buffer (containing 0.05% DM) was illuminated (>495 nm) after the dark-state spectra stabilized. (A) Then 2.5-fold of 9CR was added to the concentration of rhodopsin and mixed thoroughly. The experiment was also followed by UV-visible spectroscopy (inset A: 1, dark; 2, illuminated; 3, regenerated).

(B and C) Blue native PAGE and SDS-PAGE were performed with rhodopsin-purified PBS and in NaPi, which was expressed in HEK293S-GnTi^{-} cells. (D) The western blotting was carried out with rhodopsin, expressed in COS-1 cells, and purified in PBS, in NaPi.

related to the necessity of the presence of chloride ions, which are known to have a specific binding site in cone opsins (Wang et al., 1993). Western blot of rhodopsin in both buffers resulted in a similar smeary behavior, probably due to the glycosylation pattern of COS-1 cells (Figure 3D).

Transducin Activation of 9CR Regenerated Rhodopsin and Red Cone Opsin

To study the ability of regenerated pigments to activate transducin, purified visual pigments were tested in the dark, upon illumination, and after addition of 9CR under experimental conditions similar to those of the fluorimetric experiment (Figure 4). To do this, different sample aliquots were taken from the cuvette during the fluorimetric measurements, were added to the transducin mix immediately, and the activation was measured by means of a radioactive GTPγS^{35} binding assay. In the case of rhodopsin, an increase in transducin activation, which decreases over time, was observed immediately after photoactivation. However, the fact that upon subsequent addition of 9CR the functional activity of rhodopsin decreased may indicate regeneration of photoactivated rhodopsin with the added 9CR and formation of a dark-state pigment. Further illumination with white light of this regenerated pigment resulted in functional activation, suggesting the formation of a small amount of functionally active regenerated rhodopsin from the whole sample (Figures 4A and 4C). Importantly, the results show that photoactivated rhodopsin regenerated with 9CR is functionally active. On the other side, transducin activation of red cone opsin samples taken along the fluorescence experiment was determined as mentioned above for rhodopsin. Unlike rhodopsin, red cone opsin exhibited less ability to activate transducin than rhodopsin (Figures 4B and 4C).

Structural Comparison between Retinal Binding Sites of Rhodopsin and Red Cone Opsin with 11CR and 9CR

Two homology models for the red cone opsin were constructed based on the crystal structures of dark-state rhodopsin and opsin soaked with ATR (see the Experimental Procedures). 11CR and 9CR retinals were docked to the opsin forms of rhodopsin and of the red cone opsin. There is no structure of bovine rhodopsin available with 9CR. However, squid rhodopsin has been crystallized with both 11CR and 9CR, revealing only one minor difference between them: a shift in the localization of the C10 and C11 atoms by ~1 Å (Murakami and Kouyama, 2008, 2011). Accordingly, we assumed that the same mimicry should apply to rhodopsin and to the red cone opsin.

Figures 5A and 5B represent an initial state of 11CR or 9CR rhodopsin and red cone opsin regeneration prior to covalent binding to K296/312$^{7.43}$. Similar binding scenarios, for both retinals in both rhodopsin and red cone opsin, can be observed. According to the molecular model, a remarkable difference between the two photoreceptor proteins is the presence of W183$^{4.56}$ in red cone opsin (corresponding to C167$^{4.56}$ in rhodopsin), which may contribute to the stabilization of the retinal-opsin complexes (Nakayama et al., 1998). Therefore, W183 can help preserve the native conformation of the opsin binding pocket—in the absence of retinal—and favor increased accessibility of the retinal to red cone opsin binding pocket by favoring retinal-protein interaction. This specific Trp residue may prevent the red cone binding pocket from becoming unstructured, and it can also contribute to the large drop in fluorescence caused by 9CR in the fluorimetric experiments. The main difference between the two retinals is that the 9-*cis* isomer makes more favorable contacts with W265/281$^{6.49}$ and Y268/284$^{6.51}$ than does the 11-*cis* isomer in the two receptors in the region in the vicinity of the C13 methyl group. Thus, it is likely

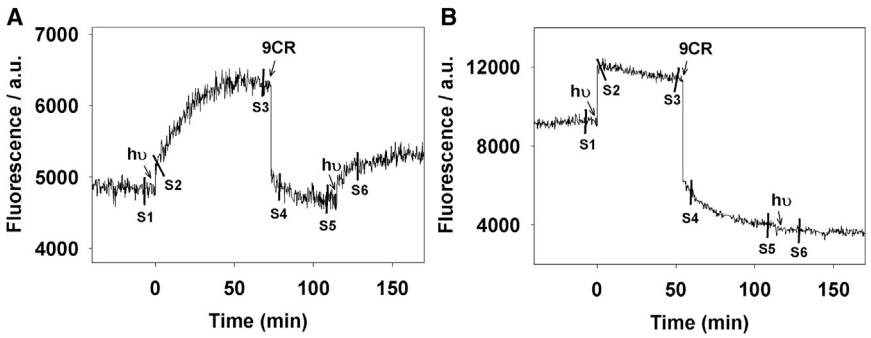

Figure 4. Transducin Activation of 9CR Regenerated Visual Pigments

(A and B) Rhodopsin and red cone opsin were monitored by means of fluorescence spectroscopy, and samples were treated by illumination ($\lambda > 495$ nm), 9CR addition, and a second illumination using white light.

(C) Rhodopsin and red cone opsin samples, taken at different time points from the experiments reported in (A) and (B) and denoted as S1–S6 (with the corresponding time in min), were analyzed for transducin activation. Each data point in (C) is represented as mean ± SD (n = 3).

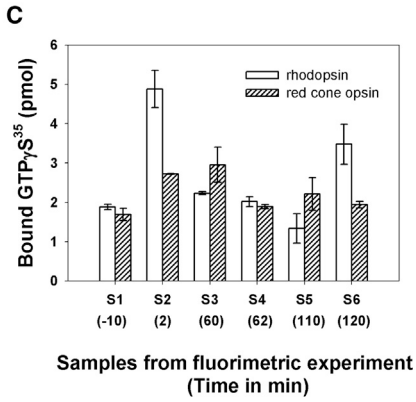

that 9CR benefits from higher stabilization energy than does 11CR in the two photoreceptors.

DISCUSSION

Active-state decay of visual photoreceptors has been extensively studied, mainly for rhodopsin but also for cone pigments. However, the receptor properties at the post-bleaching phase are still unclear. Recently, we have reported on the importance of lipids (like docosahexaenoic acid phospholipids) in the post-bleaching ability of opsin regeneration long after illumination (Sánchez-Martín et al., 2013). In that work, we reported on a decrease of fluorescence upon 11CR addition in the presence of the lipid which would reflect increased stability of the opsin molecule in the lipid environment. In the present study, our aim was to study the regeneration differences after photoactivation of purified rhodopsin and red cone opsin with two retinal analogs. Fluorescence spectroscopy has been used to track changes induced by chromophore regeneration after photoactivation and MetaII decay processes. A major finding suggests that the retinal binding site of purified recombinant rhodopsin can be accessible to 9CR a long time after illumination, but not to 11CR.

In order to understand how retinal regeneration occurs at a molecular level, it is important to understand the structural changes associated with the transition from the inactive to the active states and vice versa. In rhodopsin, K296$^{7.43}$ and W265$^{6.48}$ represent important residues of the retinal binding pocket. The aldehyde group of retinal covalently binds to K296$^{7.43}$, whereas W265$^{6.48}$ remains proximal to the β-ionone ring of retinal (Borhan et al., 2000). Comparison of the extracellular region in the dark-state (11CR-bound) and active rhodopsin structures (Li et al., 2004; Scheerer et al., 2008) (Figure 5C) shows only remarkable changes in TMs 3, 6, and 7. In specific, a decrease from 8.5 to 6.5 Å in the distance between TM5 and TM6 (measured as the distance between the α-carbons of F208$^{5.43}$ and A269$^{6.52}$). In turn, TM7 becomes closer to TM6 (from 5.5 to 4.9 Å, measured between the α-carbons of P267$^{6.50}$ and P291$^{7.51}$. On the other side, the distance between TM3 increases (from 10.7 to 13.4 Å, measured between E113$^{3.28}$ and K296$^{7.43}$). Thus, without the inverse agonist 11CR, TM6 packs more tightly with TM5. Because TM7 moves closer to TM6, the distance to TM3 increases. A major consequence of these changes is that the main countercharge of K296$^{7.43}$ changes between the dark and the active forms from E113$^{3.28}$ to E181^{C-6}. Table 1 shows a comparison between residues, forming the retinal binding sites in the rod and red cone photoreceptors. Despite the fact that they share the same endogenous ligand, only a third of the residues are conserved between rhodopsin and the red cone opsin. Crystal structures also reveal the existence of different networks of interactions close to the retinal. This suggests specific recognition mechanisms at the molecular level.

Retinal has been proposed to enter the opsin binding pocket through TM1 and TM7 (called opening A) or TMs 5 and 6 (called opening B). This opening B region is flanked by V204$^{5.39}$, F208$^{5.43}$, F212$^{5.47}$, A269$^{6.52}$, F273$^{6.56}$, and F276$^{6.59}$ (Hildebrand et al., 2009; Park et al., 2008). In the dark state, these residues constitute a zipper between the two helices that keeps the access to the protein interior closed (Figure 5D). A similar zipper is observed in the molecular model of the red cone opsin, though stabilized mainly by Met/Cys-Met/Cys interactions instead of aromatic-aromatic and aromatic-aliphatic interactions. These sulfur-containing residue interactions, which are of the same magnitude and are even stronger than aromatic-aromatic interactions, can act as molecular gears in GPCRs (Cordomí et al., 2013). In activated rhodopsin, F208$^{5.43}$ exhibits a conformational change that, together with the translation of TM5, opens a cavity within the zipper and allows the retinal into the retinal binding site (see Figures 5D and 5E). The molecular model shows clearly that this cavity is conserved in red cone opsin, except that the

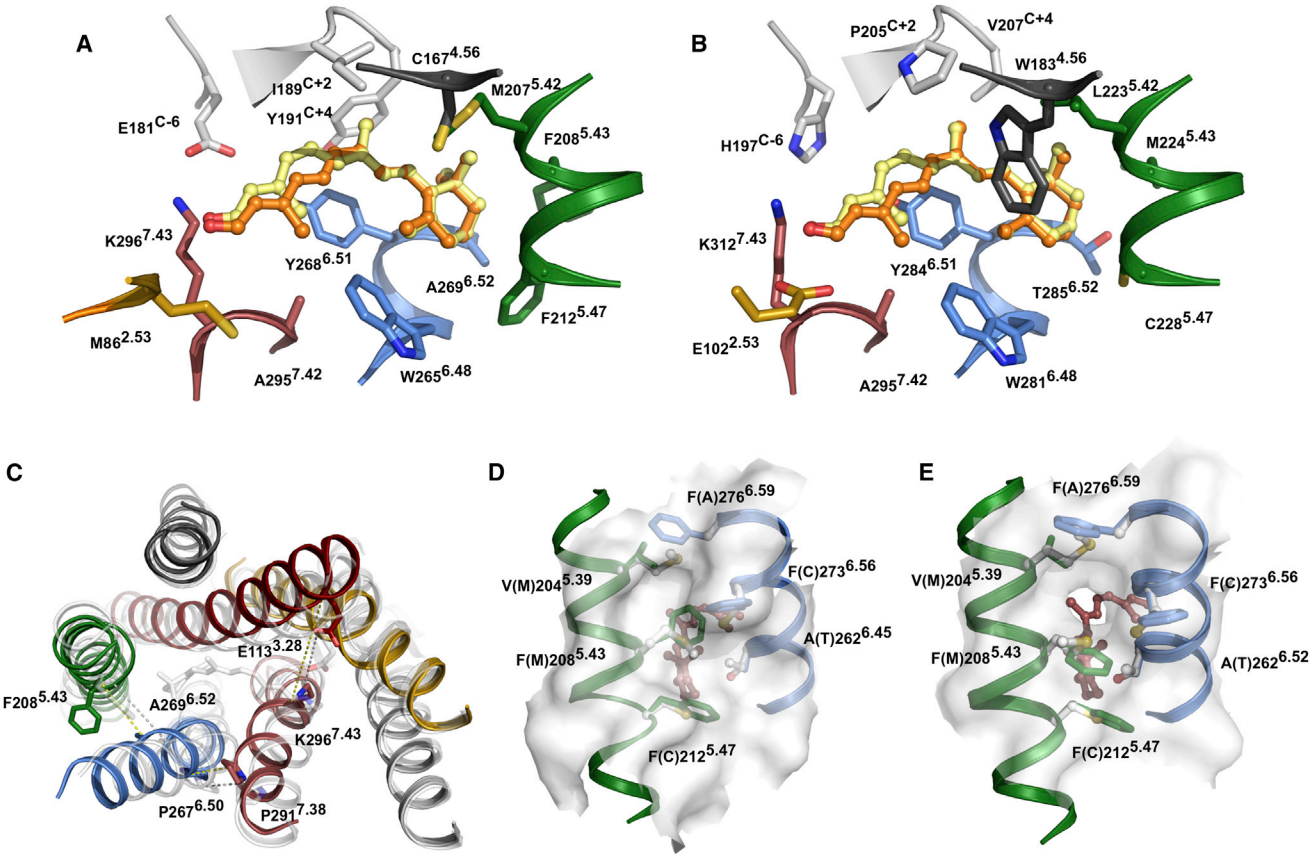

Figure 5. Molecular Models of Rhodopsin and Red Cone Opsin

(A and B) Molecular complexes for 11-*cis* (pale-yellow) and 9-*cis* (orange) retinal bound to rod (A) and red cone (B) opsins.

(C) Comparison between helical arrangements in dark-state rhodopsin (PDB ID code 1GZM, shown as white transparent cartoon) (Li et al., 2004) and opsin soaked with ATR (PDB ID code 2X72, shown as colored cartoons) (Standfuss et al., 2011). The color code for opsin helices is as follows: TM1, light gray; TM2, gold; TM3, red; TM4, dark gray; TM5, green; TM6, blue; TM7, pale red. Dashed lines display the distances between the shown amino acids (see main text; dark-state rhodopsin, white; active opsin, yellow).

(D and E) The entrance site for retinals in the dark (D) and opsin (E) states. Rod opsin residues are shown in colors, whereas residues in red cone opsin are shown in white.

opening of the zipper would be controlled by M214$^{5.43}$ instead of F208$^{5.43}$ (Figure 5E). In addition, substitution of four Phe residues by residues with smaller volume (Met, Cys, and Ala) may facilitate the entrance of retinal.

The molecular models of opsin form in complex with 11CR and 9CR, without formation of the Schiff base with K296$^{7.43}$, suggesting that 9CR benefits from stronger interactions with W265$^{6.49}$ and Y268$^{6.51}$ than does 11CR. In the red cone opsin, in addition to Y281$^{6.49}$ and W284$^{6.51}$ positions, W183$^{4.56}$ also contributes to maximal higher stabilization energy toward both retinals. The opening of TM6 after photoactivation shows that W265$^{6.49}$ presumably favors binding of 9CR, which has shorter C9 to β-ionone ring length than does 11CR. This would favor the 9-*cis* isomer to enter the retinal binding site. The previous finding that 9-demethyl retinal could inhibit the formation of active MetaII conformation of rhodopsin (Ganter et al., 1989), but not of red cone opsin (Das et al., 2004), suggests that the retinal binding site of red cone opsin is more accessible and more versatile than that of rhodopsin. The specific interaction with W265 and Y268 may contribute to enhancing 9CR fluorescence quenching. The more versatile the ligand binding site, the less constriction within the retinal entry and exit channels; hence, either retinal analog, added exogenously after photoactivation, may be accommodated into the retinal binding site, as is observed in our fluorimetric measurements.

When 11CR is added immediately after photoactivation, i.e., while MetaII intermediate of rhodopsin has not decayed yet, we observed (Figure S2) similar results to those previously published for 11CR (Farrens and Khorana, 1995), suggesting that rhodopsin is brought back to its native chromophore-regenerated state. In the case of red cone opsin, in which the $t_{1/2}$ of MetaII decay is in the milliseconds time range (Estevez et al., 2009), addition of retinal immediately after photoactivation led to a considerable decrease in Trp fluorescence, suggesting chromophore regeneration with both retinals (Figure S2). It is well established that rhodopsin regeneration ability is gradually lost with time, due to the formation of opsin conformations, which impair retinal acceptance into the binding pocket (Sakamoto and Khorana, 1995). In the case of red cone opsin, we added retinal and followed the fluorescence signal over time in

Table 1. Comparison between Residues at the Retinal Binding Pocket in Bovine Rod Opsin and in Human Red Cone Opsin

		Bovine Rhodopsin			Human Red Cone Opsin		
	BW No.[a]	Residue		Cons. (%)	Residue		Cons. (%)
TM3	3.28	Glu	113	68	Glu	129	68
	3.32	Ala	117	45	Val	133	15
	3.33	Thr	118	51	Ser	134	28
	3.37	Glu	122	38	Ile	138	27
ECL2	C−6	Glu	181	77	His	197	8
	C−1	Ser	186	80	Ser	202	80
	C+2	Ile	189	25	Pro	205	32
	C+4	Tyr	191	65	Val	207	11
TM5	5.42	Met	207	48	Leu	223	30
	5.47	Phe	212	72	Cys	228	11
TM6	6.44	Phe	261	76	Tyr	277	13
	6.48	Trp	265	92	Trp	281	92
	6.51	Tyr	268	100	Tyr	284	100
	6.52	Ala	269	70	Thr	285	11
TM7	7.39	Ala	292	74	Ala	308	74

The consensus GPCR numbering (left column) is given together with the protein-specific sequence numbering. C-i numbers indicate the position relative to the conserved cysteine in ECL2 (C187 in rhodopsin and C203 in red cone opsin). Underlined residues indicate conservation between the two proteins. Percentages of conservation (Cons.) refer to the sequence alignment of all opsins as implemented in the GPCR Motif Searcher (http://lmc.uab.cat/gmos).

[a]Ballesteros-Weinstein numbering system (Ballesteros and Weinstein, 1995).

the dark (Figure 2). Strikingly, a decrease in fluorescence was observed with either retinal, and subsequent illumination did not alter the fluorescence intensity. UV-visible spectra of the dark-state-purified visual pigments indicate that, along with the peak of regenerated pigment in the visible region, the characteristic protein peak at 280 nm can also be detected, which may account for the presence of both regenerated opsin and free opsin. At least a fraction of this opsin can be non-misfolded opsin as has already been previously reported (Jäger et al., 1996; Reeves et al., 1999). The A_{280}/A_{560} ratio of red cone opsin, from the UV-visible spectrum, indicates the presence of non-regenerated opsin in the eluted purified sample. We suggest that the decrease in fluorescence observed in both red cone opsin and rhodopsin, in the dark before photoactivation, is due to the presence of free opsin that can accept the exogenously added free retinal. The lack of a classical photoresponse upon illumination (Figure 2) can be explained by the presence of excess free retinal in the sample. Interestingly, a saturation curve is obtained upon hydroxylamine addition, which may reflect additional retinal release from the binding pocket. The $t_{1/2}$ of this process is ~3 min, and this parameter can be used to assess the regeneration properties of red cone opsin mutants (associated with visual disorders) that we are currently studying. The observation of similar features in the case of rhodopsin with the addition of 9CR—except the fact of faster formation of retinaloxime—and the lack of effect with 11CR conclusively supports the hypothesis that the binding pocket of free opsin from rhodopsin can be accessible by 9CR, but not by 11CR, under our experimental conditions. A recent study on the thermal properties of rhodopsin reports that exogenous addition of 11CR 10 min after photoactivation shows a decrease in Trp fluorescence intensity, which is 20% of the total fluorescence increase observed after photobleaching. However, the conditions used in this study are different from those in the present study, namely, that they used a 1:1 retinal:opsin ratio, a temperature of 55°C and a shorter post-bleaching time (Liu et al., 2011).

We performed BN-PAGE in order to identify the presence of rhodopsin oligomeric forms in different buffers (Shukolyukov, 2009). Higher molecular weight bands—corresponding to oligomeric forms of rhodopsin—appear to be more intense in NaPi (Figure 3B). These oligomeric forms of rhodopsin may favor post-bleaching regeneration of rhodopsin, due to increased stability provided by dimeric opsin units. The differences in oligomerization may account for the different kinetics observed for rhodopsin regeneration in PBS and NaPi buffers. Recent studies have highlighted the influence of rhodopsin dimers on its capacity for regeneration with either 11CR or 9CR (Jastrzebska et al., 2013b) and on the asymmetry of the rhodopsin dimer complex with transducin (Jastrzebska et al., 2013a). Attempts to purify regenerated red cone opsin using NaPi buffer were unsuccessful. Thus, regenerated red cone opsin can only be obtained in PBS buffer, consistent with the fact that a chloride binding site is crucial for the optimal conformation of cone pigments (Wang et al., 1993).

Overall, the observed different regeneration ability of rhodopsin and red cone opsin, with 9CR and 11CR, may be due to a combination of both stability and accessibility effects. These two effects may explain the differences observed for the two visual pigments. In the case of samples in PBS buffer, the opsin protein would show lower stability—being predominantly monomeric—and this would alter the conformation of the retinal binding pocket, thus affecting the accessibility of retinal to the pocket. When the protein is in NaPi, the presence of dimers would help stabilizing opsin, and this would better preserve the correct retinal binding conformation facilitating accessibility of retinal to the interior of the protein. Therefore, increased stability of the opsin retinal binding pocket structure would result in better retinal.

On the functional side, rhodopsin appears to activate rod transducin more effectively than red cone opsin. This result is in line with a recent study in which transducin activation by cone pigment is slowed immediately after photoactivation in contrast to the rhodopsin behavior (Imamoto et al., 2013).

SIGNIFICANCE

The findings of the present study indicate that the constricted retinal binding site of rhodopsin (together with an inherently less-stable retinal binding pocket in the opsin conformation) restricts the entry of 11CR but permits the entry of 9CR into the retinal binding site a long time after photoactivation. In contrast, the flexible (and more stable in the opsin state) retinal binding site of red cone opsin is open to the entry of either retinal isomer. In red cone opsin, both retinals benefit from the interaction with W183$^{4.56}$ (lacking in rhodopsin), which favors the entry of 11CR and 9CR into the retinal binding site. However, 9CR interacts more favorably than 11CR with Y268/284$^{6.51}$ and W265/281$^{6.48}$. This

would be justified by the stronger interaction energy acquired by the C-13 methyl group of 9CR from Y268 and W265, favoring the entry into the rhodopsin retinal binding site, which is lower in the case of the 11CR ligand. Functional activity of the pigments, regenerated with 9CR after photoactivation, has been also detected for both receptors. Red cone opsin appears to activate rod transducin less efficiently, which would be consistent with the known physiological response for cone pigments. Thus, our results, on the specific ligand/receptor interactions described, highlight the tight coupling of the ligands with their receptors after activation and also suggest that the oligomerization state of rhodopsin modulates the retinal-opsin binding processes. These effects can certainly play an important role in the activation process of GPCRs, not only of other rhodopsin-like GPCRs but of other subfamilies of GPCRs as well.

EXPERIMENTAL PROCEDURES

Materials

The red cone opsin gene, cloned into pMT4 plasmid vector, was kindly provided by Prof. Kevin D. Ridge. Dulbecco's modified Eagle medium (PAA Laboratories), supplemented with fetal bovine serum (Sigma), L-glutamine (Sigma), and penicillin-streptomycin (Sigma), was used to culture COS-1 cells (American Type Culture Collection no. CRL-1650). 11CR was provided by the National Eye Institute, National Institutes of Health. Purified mAb rho-1D4 was obtained from Cell Essentials and was coupled to CNBr-activated Sepharose beads (Sigma). n-dodecyl-β-D-maltoside (DM) was purchased from Affymetrix. The nonamer-peptide H-TETSQVAPA-OH was obtained from Unitat de Tècniques Separatives i Síntesi de Pèptids, Universitat de Barcelona. 9CR, hydroxylamine, protease inhibitor cocktail, and phenylmethanesulfonyl fluoride (PMSF) were purchased from Sigma, and polyethyleneimine (PEI) was purchased from Polysciences. Cellulose membrane used for the G protein activation assay was purchased from Millipore.

Methods

Expression and Purification of Rhodopsin and Red Cone Opsin

Rhodopsin or red cone opsin genes were expressed in transiently transfected COS-1 cells by chemical transfection using PEI reagent. Cells were harvested 48–60 hr after transfection and regenerated with 10 μM 11CR in PBS buffer (137 mM NaCl, 2.7 mM KCl, 10 mM Na_2HPO_4, and 1.8 mM KH_2PO_4 [pH 7.4]) by overnight incubation at 4°C. Regenerated cells were subsequently solubilized using 1% DM with PMSF and protease inhibitors, and the pigments were purified by immunoaffinity chromatography using Sepharose coupled to rho-1D4 antibody. The bound rhodopsin and red cone opsin were eluted in PBS containing the nonamer peptide and 0.05% DM. COS-1 cells were used for the expression of the recombinant proteins in all experiments, except for samples used in the electrophoretic analysis.

Characterization of Regenerated Rhodopsin and Cone Opsin by UV-Visible Spectroscopy

Purified pigments were spectroscopically characterized using a Varian Cary 100 Bio spectrophotometer (Varian), equipped with a water-jacketed cuvette holder connected to a circulating water bath. Temperature was controlled by a peltier accessory connected to the spectrophotometer. All the spectra were recorded in the 250–650 nm range for rhodopsin and 250–700 nm for red cone opsin, with a bandwidth of 2 nm, a response time of 0.5 s, and a scan speed of 400 nm/min.

Fluorescence Spectroscopy of Retinal Release and Regeneration after Photoactivation

QuantaMaster 4 spectrofluorimeter (Proton Technology International) was employed to measure the Trp fluorescence emission corresponding to retinal release and uptake processes. The excitation wavelength was 295 nm, and the emission wavelength was 330 nm, measuring 1 point per second for 2 s, followed by a 28 s pause (with a beam shutter to prevent sample photobleaching by the fluorimeter lamp). The excitation slit settings were 0.5 nm, and emission was 10 nm. Trp fluorescence was monitored over time in the dark until a steady baseline was obtained. Then the sample was photobleached with a 495 nm cut-off filter for 30 s using a Dolan-Jenner MI-150 fiber-optic illuminator, and the change in fluorescence was recorded. For regeneration experiments, a 2.5-fold molar concentration of retinal over pigment was used. The volume of the retinal stock added to the protein sample was 1% of the total sample volume.

BN-PAGE

BN-PAGE was performed as previously described (Schägger and von Jagow, 1991; Wittig et al., 2006), with a few modifications. For electrophoresis, a Bio-Rad Mini-PROTEAN 2 gel running apparatus was used with the corresponding gel running buffer (50 mM Tricine, 15 mM Bi-Tris, and 0.02% Coomassie blue G [pH 7.0]). The gel was casted with the separating gel (13% acrylamide, 50 mM bis-Tris, 1.2% ammonium persulfate, and 0.6% TEMED) and stacking gel (4.2% acrylamide, 15 mM bis-Tris, 1% ammonium persulfate, and 1% TEMED). Here, the rhodopsin gene was expressed in transiently transfected HEK293S-GnTi$^-$ cells—which lack glycosylation—in order to avoid the smeary appearance of protein bands by difference in glycosylation patterns (Reeves et al., 2002). Rhodopsin concentrations of purified samples, using PBS and NaPi (2 mM sodium dihydrogen phosphate and disodium hydrogen phosphate mixed to pH 7.4), were normalized using $A_{280\ nm}$ in the UV-visible spectra. An equal amount of protein samples in sample buffer (5% glycerol and 0.01% Ponceau-Red) were loaded onto the gel, which was destained and visualized after 4 hr.

SDS-PAGE

Equal amounts of rhodopsin samples, purified in PBS and NaPi buffers, were used to carry out SDS-PAGE as described earlier (Laemmli, 1970).

Western Blot Analysis

Rhodopsin, purified either in PBS or in NaPi buffer, was used for SDS-PAGE. The proteins from the gel were transferred onto a nitrocellulose membrane and detected using 1:10,000 dilution of the rho-1D4 anti-mouse antibody and 1:5,000 dilution of goat anti-mouse IgG conjugated to horseradish peroxidase (Santa Cruz Biotechnology). The blots were developed using substrate Super-Signal West Pico Chemiluminescent Substrate (Luminol/H2O2) (Thermo Fisher Scientific).

Transducin Activation Assay

Transducin was purified from bovine retinas and stored in 20 mM Tris (pH 7.5), 100 mM NaCl, 50% glycerol, 10 mM β-mercaptoethanol, and 5 mM magnesium acetate as previously described (Fukada et al., 1994). For the transducin activation assay, 10 nM pigment aliquots (~1–2 μl) were taken from the same sample used in the spectrofluorimetric experiment, at different time points, in order to ensure that the conditions of the assay were identical in both cases, thus allowing reliable correlation between the two data sets. The samples were added to a mixture of 500 nM transducin in assay buffer (25 mM Tris [pH 7.5], 5 mM $MgCl_2$, 100 mM NaCl, 2.5 mM dithiothreitol, and 0.013% DM) containing 5 μM GTPγS^{35} (0.156 mCi/mmol). The reaction mixture was incubated at room temperature for 20 min in the dark and transferred onto a 96-well cellulose membrane plate. The plate was fixed to a manifold filtering unit, and the membrane was washed thoroughly with assay buffer. Bound GTPγS^{35} was measured by means of a Tri Carb 2100TR liquid scintillation counter (PerkinElmer).

Molecular Model of Rhodopsin and Red Cone Opsin

The sequences of bovine rhodopsin (P02699) and human red opsin (P04000) were retrieved from Uniprot (UniProt Consortium, 2010) and aligned. Excluding the first 15 and 31 residues of the N terminus of rhodopsin and red-opsin, respectively, the sequence identity between bovine rhodopsin and human red opsin is 39%, and sequence similarity reaches 55%. The alignment between the two sequences did not contain any gap. Thus, it is possible to create reliable models for the human red opsin based on bovine rhodopsin even for loops. Homology models for the dark-state and active human red opsin were constructed, respectively, based on the crystal structure of bovine rhodopsin (Protein Data Bank [PDB] ID code 1GZM) (Li et al., 2004) and the opsin soaked with *ATR* (PDB ID code 2X72) (Scheerer et al., 2008). Modeler (v. 9.8) was used for this purpose (Sali and Blundell, 1993).

Molecular Models of the Regenerated Photoreceptors with 11CR and 9CR

The photoreceptors with 11CR and 9CR, mimicking the regeneration process, were modeled using the rhodopsin structure containing retinal without

formation of the Schiff base with K296$^{7.43}$ (PDB ID code 2X72) (Standfuss et al., 2011). 11CR and 9CR were manually docked in the same volume occupied by the unbound ATR. Four complexes combining rhodopsin and red opsin with 11CR and 9CR were constructed and refined using energy minimization with the AMBER program (Case et al., 2012). The force field Amberff99SB-ILDN was employed in all simulations (Lindorff-Larsen et al., 2010).

Statistical Analysis

The error bars are represented as mean ± SD (n = 3).

SUPPLEMENTAL INFORMATION

Supplemental Information includes three figures and can be found with this article online at http://dx.doi.org/10.1016/j.chembiol.2014.01.006.

ACKNOWLEDGMENTS

This work was supported by the Ministerio de Ciencia e Innovación (Spain) (SAF2011-30216-C02-01), by Grups de Recerca Consolidats de la Generalitat de Catalunya (2009 SGR 1402), and by Fundación Ramón Areces (to P.G.) and by a CIG grant from the European Commission (to E.R.). S.S. is the recipient of a FI-AGAUR Fellowship, and E.R. is the recipient of a Beatriu de Pinós Fellowship from AGAUR. A.C. is the recipient of a contract grant from the Instituto de Salud Carlos III.

Received: October 25, 2013
Revised: December 21, 2013
Accepted: January 13, 2014
Published: February 20, 2014

REFERENCES

Ballesteros, J.A., and Weinstein, H. (1995). Integrated methods for the construction of three-dimensional models and computational probing of structure-function relations in G protein-coupled receptors. Methods in Neurosciences *25*, 366–428.

Bartl, F.J., Fritze, O., Ritter, E., Herrmann, R., Kuksa, V., Palczewski, K., Hofmann, K.P., and Ernst, O.P. (2005). Partial agonism in a G Protein-coupled receptor: role of the retinal ring structure in rhodopsin activation. J. Biol. Chem. *280*, 34259–34267.

Borhan, B., Souto, M.L., Imai, H., Shichida, Y., and Nakanishi, K. (2000). Movement of retinal along the visual transduction path. Science *288*, 2209–2212.

Case, D.A., Darden, T.A., Cheatham, T.E., III, Simmerling, C.L., Wang, J., Duke, R.E., Luo, R., Walker, R.C., Zhang, W., Merz, K.M., Roberts, B., Hayik, S., Roitberg, A., Seabra, G., Swails, J., Goetz, A.W., Kolossváry, I., Wong, K.F., Paesani, F., Vanicek, J., Wolf, R.M., Liu, J., Wu, X., Brozell, S.R., Steinbrecher, T., Gohlke, H., Cai, Q., Ye, X., Wang, J., Hsieh, M.-J., Cui, G., Roe, D.R., Mathews, D.H., Seetin, M.G., Salomon-Ferrer, R., Sagui, C., Babin, V., Luchko, T., Gusarov, S., Kovalenko, A., and Kollman, P.A. (2012). AMBER 12. (San Francisco: University of California, San Francisco).

Chen, M.H., Kuemmel, C., Birge, R.R., and Knox, B.E. (2012). Rapid release of retinal from a cone visual pigment following photoactivation. Biochemistry *51*, 4117–4125.

Cordomí, A., Gómez-Tamayo, J.C., Gigoux, V., and Fourmy, D. (2013). Sulfur-containing amino acids in 7TMRs: molecular gears for pharmacology and function. Trends Pharmacol. Sci. *34*, 320–331.

Das, J., Crouch, R.K., Ma, J.X., Oprian, D.D., and Kono, M. (2004). Role of the 9-methyl group of retinal in cone visual pigments. Biochemistry *43*, 5532–5538.

Estevez, M.E., Kolesnikov, A.V., Ala-Laurila, P., Crouch, R.K., Govardovskii, V.I., and Cornwall, M.C. (2009). The 9-methyl group of retinal is essential for rapid Meta II decay and phototransduction quenching in red cones. J. Gen. Physiol. *134*, 137–150.

Farrens, D.L., and Khorana, H.G. (1995). Structure and function in rhodopsin. Measurement of the rate of metarhodopsin II decay by fluorescence spectroscopy. J. Biol. Chem. *270*, 5073–5076.

Fukada, Y., Okano, T., Shichida, Y., Yoshizawa, T., Trehan, A., Mead, D., Denny, M., Asato, A.E., and Liu, R.S. (1990). Comparative study on the chromophore binding sites of rod and red-sensitive cone visual pigments by use of synthetic retinal isomers and analogues. Biochemistry *29*, 3133–3140.

Fukada, Y., Matsuda, T., Kokame, K., Takao, T., Shimonishi, Y., Akino, T., and Yoshizawa, T. (1994). Effects of carboxyl methylation of photoreceptor G protein gamma-subunit in visual transduction. J. Biol. Chem. *269*, 5163–5170.

Ganter, U.M., Schmid, E.D., Perez-Sala, D., Rando, R.R., and Siebert, F. (1989). Removal of the 9-methyl group of retinal inhibits signal transduction in the visual process. A Fourier transform infrared and biochemical investigation. Biochemistry *28*, 5954–5962.

Harbison, G.S., Smith, S.O., Pardoen, J.A., Winkel, C., Lugtenburg, J., Herzfeld, J., Mathies, R., and Griffin, R.G. (1984). Dark-adapted bacteriorhodopsin contains 13-cis, 15-syn and all-trans, 15-anti retinal Schiff bases. Proc. Natl. Acad. Sci. USA *81*, 1706–1709.

Hildebrand, P.W., Scheerer, P., Park, J.H., Choe, H.W., Piechnick, R., Ernst, O.P., Hofmann, K.P., and Heck, M. (2009). A ligand channel through the G protein coupled receptor opsin. PLoS ONE *4*, e4382.

Hoersch, D., Otto, H., Wallat, I., and Heyn, M.P. (2008). Monitoring the conformational changes of photoactivated rhodopsin from microseconds to seconds by transient fluorescence spectroscopy. Biochemistry *47*, 11518–11527.

Hubbard, R., and Wald, G. (1952). Cis-trans isomers of vitamin A and retinene in the rhodopsin system. J. Gen. Physiol. *36*, 269–315.

Imai, H., Terakita, A., Tachibanaki, S., Imamoto, Y., Yoshizawa, T., and Shichida, Y. (1997). Photochemical and biochemical properties of chicken blue-sensitive cone visual pigment. Biochemistry *36*, 12773–12779.

Imamoto, Y., Seki, I., Yamashita, T., and Shichida, Y. (2013). Efficiencies of activation of transducin by cone and rod visual pigments. Biochemistry *52*, 3010–3018.

Jäger, S., Palczewski, K., and Hofmann, K.P. (1996). Opsin/all-trans-retinal complex activates transducin by different mechanisms than photolyzed rhodopsin. Biochemistry *35*, 2901–2908.

Jastrzebska, B., Orban, T., Golczak, M., Engel, A., and Palczewski, K. (2013a). Asymmetry of the rhodopsin dimer in complex with transducin. FASEB J. *27*, 1572–1584.

Jastrzebska, B., Ringler, P., Palczewski, K., and Engel, A. (2013b). The rhodopsin-transducin complex houses two distinct rhodopsin molecules. J. Struct. Biol. *182*, 164–172.

Kakitani, H., Kakitani, T., Rodman, H., and Honig, B. (1985). On the mechanism of wavelength regulation in visual pigments. Photochem. Photobiol. *41*, 471–479.

Kawamura, S., and Tachibanaki, S. (2008). Rod and cone photoreceptors: molecular basis of the difference in their physiology. Comp. Biochem. Physiol. A Mol. Integr. Physiol. *150*, 369–377.

Laemmli, U.K. (1970). Cleavage of structural proteins during the assembly of the head of bacteriophage T4. Nature *227*, 680–685.

Li, J., Edwards, P.C., Burghammer, M., Villa, C., and Schertler, G.F.X. (2004). Structure of bovine rhodopsin in a trigonal crystal form. J. Mol. Biol. *343*, 1409–1438.

Lindorff-Larsen, K., Piana, S., Palmo, K., Maragakis, P., Klepeis, J.L., Dror, R.O., and Shaw, D.E. (2010). Improved side-chain torsion potentials for the Amber ff99SB protein force field. Proteins *78*, 1950–1958.

Liu, J., Liu, M.Y., Nguyen, J.B., Bhagat, A., Mooney, V., and Yan, E.C. (2011). Thermal properties of rhodopsin: insight into the molecular mechanism of dim-light vision. J. Biol. Chem. *286*, 27622–27629.

Matsuyama, T., Yamashita, T., Imai, H., and Shichida, Y. (2010). Covalent bond between ligand and receptor required for efficient activation in rhodopsin. J. Biol. Chem. *285*, 8114–8121.

Merbs, S.L., and Nathans, J. (1992). Absorption spectra of human cone pigments. Nature *356*, 433–435.

Murakami, M., and Kouyama, T. (2008). Crystal structure of squid rhodopsin. Nature *453*, 363–367.

Murakami, M., and Kouyama, T. (2011). Crystallographic analysis of the primary photochemical reaction of squid rhodopsin. J. Mol. Biol. *413*, 615–627.

Mustafi, D., Engel, A.H., and Palczewski, K. (2009). Structure of cone photoreceptors. Prog. Retin. Eye Res. *28*, 289–302.

Nakamichi, H., and Okada, T. (2007). X-ray crystallographic analysis of 9-cis-rhodopsin, a model analogue visual pigment. Photochem. Photobiol. *83*, 232–235.

Nakayama, T.A., Zhang, W., Cowan, A., and Kung, M. (1998). Mutagenesis studies of human red opsin: trp-281 is essential for proper folding and protein-retinal interactions. Biochemistry *37*, 17487–17494.

Neitz, M., Neitz, J., and Jacobs, G.H. (1991). Spectral tuning of pigments underlying red-green color vision. Science *252*, 971–974.

Palczewski, K., Kumasaka, T., Hori, T., Behnke, C.A., Motoshima, H., Fox, B.A., Le Trong, I., Teller, D.C., Okada, T., Stenkamp, R.E., et al. (2000). Crystal structure of rhodopsin: a G protein-coupled receptor. Science *289*, 739–745.

Park, J.H., Scheerer, P., Hofmann, K.P., Choe, H.W., and Ernst, O.P. (2008). Crystal structure of the ligand-free G-protein-coupled receptor opsin. Nature *454*, 183–187.

Ramon, E., del Valle, L.J., and Garriga, P. (2003). Unusual thermal and conformational properties of the rhodopsin congenital night blindness mutant Thr-94 → Ile. J. Biol. Chem. *278*, 6427–6432.

Reeves, P.J., Hwa, J., and Khorana, H.G. (1999). Structure and function in rhodopsin: kinetic studies of retinal binding to purified opsin mutants in defined phospholipid-detergent mixtures serve as probes of the retinal binding pocket. Proc. Natl. Acad. Sci. USA *96*, 1927–1931.

Reeves, P.J., Kim, J.M., and Khorana, H.G. (2002). Structure and function in rhodopsin: a tetracycline-inducible system in stable mammalian cell lines for high-level expression of opsin mutants. Proc. Natl. Acad. Sci. USA *99*, 13413–13418.

Reyes-Alcaraz, A., Martínez-Archundia, M., Ramon, E., and Garriga, P. (2011). Salt effects on the conformational stability of the visual G-protein-coupled receptor rhodopsin. Biophys. J. *101*, 2798–2806.

Sakamoto, T., and Khorana, H.G. (1995). Structure and function in rhodopsin: the fate of opsin formed upon the decay of light-activated metarhodopsin II in vitro. Proc. Natl. Acad. Sci. USA *92*, 249–253.

Sali, A., and Blundell, T.L. (1993). Comparative protein modelling by satisfaction of spatial restraints. J. Mol. Biol. *234*, 779–815.

Sánchez-Martín, M.J., Ramon, E., Torrent-Burgués, J., and Garriga, P. (2013). Improved conformational stability of the visual G protein-coupled receptor rhodopsin by specific interaction with docosahexaenoic acid phospholipid. ChemBioChem *14*, 639–644.

Schägger, H., and von Jagow, G. (1991). Blue native electrophoresis for isolation of membrane protein complexes in enzymatically active form. Anal. Biochem. *199*, 223–231.

Scheerer, P., Park, J.H., Hildebrand, P.W., Kim, Y.J., Krauss, N., Choe, H.W., Hofmann, K.P., and Ernst, O.P. (2008). Crystal structure of opsin in its G-protein-interacting conformation. Nature *455*, 497–502.

Schertler, G.F. (2008). Signal transduction: the rhodopsin story continued. Nature *453*, 292–293.

Schick, G.A., Cooper, T.M., Holloway, R.A., Murray, L.P., and Birge, R.R. (1987). Energy storage in the primary photochemical events of rhodopsin and isorhodopsin. Biochemistry *26*, 2556–2562.

Schoenlein, R.W., Peteanu, L.A., Mathies, R.A., and Shank, C.V. (1991). The first step in vision: femtosecond isomerization of rhodopsin. Science *254*, 412–415.

Shichida, Y., and Imai, H. (1998). Visual pigment: G-protein-coupled receptor for light signals. Cell. Mol. Life Sci. *54*, 1299–1315.

Shukolyukov, S.A. (2009). Aggregation of frog rhodopsin to oligomers and their dissociation to monomer: application of BN- and SDS-PAGE. Biochemistry Mosc. *74*, 599–604.

Standfuss, J., Edwards, P.C., D'Antona, A., Fransen, M., Xie, G., Oprian, D.D., and Schertler, G.F. (2011). The structural basis of agonist-induced activation in constitutively active rhodopsin. Nature *471*, 656–660.

Toledo, D., Cordomí, A., Proietti, M.G., Benfatto, M., del Valle, L.J., Pérez, J.J., Garriga, P., and Sepulcre, F. (2009). Structural characterization of a zinc high-affinity binding site in rhodopsin. Photochem. Photobiol. *85*, 479–484.

Toledo, D., Ramon, E., Aguilà, M., Cordomí, A., Pérez, J.J., Mendes, H.F., Cheetham, M.E., and Garriga, P. (2011). Molecular mechanisms of disease for mutations at Gly-90 in rhodopsin. J. Biol. Chem. *286*, 39993–40001.

UniProt Consortium (2010). The Universal Protein Resource (UniProt) in 2010. Nucleic Acids Res. *38* (Database issue), D142–D148.

Wald, G. (1968). Molecular basis of visual excitation. Science *162*, 230–239.

Wang, Z., Asenjo, A.B., and Oprian, D.D. (1993). Identification of the Cl(−)-binding site in the human red and green color vision pigments. Biochemistry *32*, 2125–2130.

Wittig, I., Braun, H.P., and Schägger, H. (2006). Blue native PAGE. Nat. Protoc. *1*, 418–428.

Zhukovsky, E.A., Robinson, P.R., and Oprian, D.D. (1991). Transducin activation by rhodopsin without a covalent bond to the 11-*cis*-retinal chromophore. Science *251*, 558–560.